

Journal of Materials Chemistry C

Accepted Manuscript



This is an *Accepted Manuscript*, which has been through the Royal Society of Chemistry peer review process and has been accepted for publication.

Accepted Manuscripts are published online shortly after acceptance, before technical editing, formatting and proof reading. Using this free service, authors can make their results available to the community, in citable form, before we publish the edited article. We will replace this *Accepted Manuscript* with the edited and formatted *Advance Article* as soon as it is available.

You can find more information about *Accepted Manuscripts* in the [Information for Authors](#).

Please note that technical editing may introduce minor changes to the text and/or graphics, which may alter content. The journal's standard [Terms & Conditions](#) and the [Ethical guidelines](#) still apply. In no event shall the Royal Society of Chemistry be held responsible for any errors or omissions in this *Accepted Manuscript* or any consequences arising from the use of any information it contains.

New Spirobifluorene Based Hole-Transporting Semiconductors for Electroluminescent Devices

Özlem Usluer^{1*}

¹Department of Chemistry, Muğla Sıtkı Koçman University, 48000, Muğla, Turkey

*Correspondence to: Özlem Usluer (e-mail:usluerozlem@yahoo.com.tr)

Abstract

A series of spirofluorene-centered, carbazole and thiophene -linked molecules CFT, TCFT and CFTFC were synthesized by Ulmann coupling and Suzuki Cross-coupling reactions and fully characterized by ¹H NMR, ¹³C NMR, FTIR, UV-vis, PL spectroscopy, DSC, TGA, CV and MALDI-TOF. Multilayer organic light-emitting diode (OLED) devices based on these materials were fabricated to investigate their hole-transport properties. Electroluminescent properties of these molecules showed excellent performance in devices. CFT-based OLED devices exhibited the best performance with a low turn on voltage of 3 V, a maximum luminance of 10100 cd/m² and a maximum luminous efficiency of 11.30 (cd/A). This work brings opportunities for the employment of spirobifluorene semiconductors for use in highly efficient OLED applications.

Keywords: Organic light-emitting diode, hole transport layer, carbazole, fluorene, thiophene

Introduction

Organic light emitting diodes (OLEDs) have attracted much attention due to their potential application in full-color flatpanel displays and solid lighting resources.¹⁻⁴ Since the initial work on small molecular OLEDs by Tang *et al.* and polymer light emitting diodes (PLEDs) by Burroughes *et al.*, many researchers focused on the development of electroluminescent materials with high luminescent efficiency, better stabilities, and good film forming properties to improve device efficiency and enhancing the durability of OLEDs.^{5,9}

Fluorene- based compounds are desirable materials for organic optoelectronic devices, such as light-emitting diodes,¹⁰ photovoltaic cells,¹¹ field-effect transistors,¹² and organic lasers,¹³ owing to their high thermal and morphological stabilities, high fluorescent quantum efficiencies, and ambipolar carrier transporting properties.¹⁴ In recent years, polyfluorene derivatives have been broadly used in PLEDs because of their high efficiencies both in photoluminescence (PL) and in electroluminescence (EL) devices.^{15,16} However, the 9,9-dialkylated fluorene derivatives have shown poor spectral stabilities associated with keto

defects in the polymer backbone or excimer emission.¹⁷ 9,9-Spirobifluorene derivatives have also attracted much attention due to their solution processability, high luminescence efficiency and their morphologic stability.¹⁸ Spiroannulated molecules utilize the spiro bridge to connect two conjugated moieties via a tetrahedral bonding atom at the center. This structure minimizes the probability of interchain interactions, prevents the close packing of the molecules, increases the rigidity and glass transition temperatures (T_g).¹⁹ On the other hand, carbazole derivatives have been extensively studied because of their excellent hole-transporting capability, high charge carrier mobility, high thermal, morphological and photochemical stability.²⁰⁻²² Carbazole based compounds can be used in OLEDs as hole transporting materials,²³ host materials,²⁴ blue emitters,²⁵ green emitters,²⁶ red emitters²⁷ and white emitters.²⁸

This report describes the synthesis, characterization and application of new spirobifluorene based molecules CFT, TCFT and CFTFC as hole-transporting materials (HTMs) in organic light emitting diodes. CFT, TCFT and CFTFC were synthesized using Ullmann coupling and Suzuki Cross-coupling methods. Their chemical structures were elucidated by ^1H NMR, ^{13}C NMR, FTIR and MALDI-TOF. Photophysical, electrochemical and thermal properties of these molecules were determined by UV-Vis and PL techniques, cyclic voltammetry (CV), thermogravimetric analysis (TGA) and differential scanning calorimetry (DSC). In order to investigate their hole-transporting properties, multilayer OLED devices were fabricated with the following configuration: ITO/PEDOT:PSS/HTL/Alq3/LiF:Al. Hole-transporting abilities of the synthesized molecules were compared with the commercial hole transport material PVK in the same device architecture.

Experimental

Materials and Instruments

All reagents and solvents were purchased from Aldrich and used without further purification. Alq3, PEDOT:PSS and Indium tin oxide (ITO)-covered glass plates for EL device fabrication were obtained from Aldrich, H.C. Starck and Kintec Company, respectively.

^1H and ^{13}C NMR spectra were recorded with a Bruker 400 MHz spectrometer with chloroform- d as solvent and tetramethylsilane as the internal standard. FTIR spectra were recorded by a Perkin Elmer FTIR Spectrum One by using ATR system (4000–650 cm^{-1}). Absorption spectra were recorded on a LAMBDA 16 spectrophotometer (Perkin Elmer). Fluorescence emission and excitation spectra were measured using a LS50B luminescence spectrometer (Perkin Elmer). Electrochemical measurements were performed using a

CHI660B electrochemical workstation from CH Instruments (Austin, TX, U.S.A.). A conventional three-electrode configuration in 0.1 M solution of tetrabutylammonium hexafluorophosphate dissolved in acetonitrile:dichloromethane (2:1; v:v) at a scan rate of 100 mV s⁻¹ with a platinum working electrode, a Pt-wire counter electrode, and an Ag/AgCl reference electrode were used. Differential scanning calorimetry (DSC) measurement and thermogravimetric analysis (TGA) were performed under a nitrogen atmosphere at a heating rate of 10 °C min⁻¹, on Perkin Elmer Pyris 6 DSC and Perkin Elmer Pyris 6 TGA, respectively. MALDI-TOF spectrum was recorded by using Applied Biosystems Voyager System 6020.

Synthesis

Synthesis of 9-biphenyl-2-yl-2-bromo-7-iodo-9H-fluoren-9-ol (3): Under argon atmosphere, 2-bromobiphenyl (4.0 g, 16.5 mmol) was added slowly to magnesium turnings (0.5 g, 20.8 mmol) in freshly distilled tetrahydrofuran (THF) (15 mL). The addition was carried out in such a way that the solution maintained a gentle reflux. After the completion of addition, the mixture was diluted with dry THF (15 mL) and heated to reflux for 1 h. Then a solution of 2-bromo-7-iodo-fluoren-9-one (7.69 g, 20 mmol) dissolved in dry tetrahydrofuran (50 mL) was added to the refluxing solution of 2-biphenylmagnesium bromide in a dropwise fashion. The final mixture was heated to reflux 24 h. After cooling, the mixture was slowly added to a saturated solution of ammonium chloride (200 mL), mixed vigorously for 1 h, diluted by adding THF (50 mL), and ethyl acetate (100 mL). After separation of the phases, the aqueous part was extracted with diethyl ether (2 × 100 mL). The combined organic phase was further washed with diionized water (2 × 100 mL), brine (100 mL) and dried over magnesium sulfate. Removal of the organic solvent under vacuum gave **3** (6.22 g, 70%) as a white solid.

Synthesis of 2-bromo-7-iodo-9,9'-spirobi[fluorene] (4): A solution of **3** (5.0 g, 9.27 mmol) in dichloromethane (200 mL) was acidified by adding methanesulfonic acid (5 mL) and refluxed for 1 h. After cooling to room temperature, the solution was extracted with saturated potassium carbonate (2 × 200 mL) and washed with brine (2 × 200 mL). Solvent was removed by rotary evaporator, the resulting viscous oil was further dried under high vacuum to produce **4** (4.4 g, 92%) as a white crystalline solid and was used in the next step without purification. ¹H NMR (400 MHz, CDCl₃, 25 °C, TMS): δ (ppm) = 7.85-7.84 (d, 2H), 7.70-7.65 (t, 2H), 7.56-7.54 (d, 1H), 7.49-7.47 (dd, 1H), 7.42-7.38 (t, 2H), 7.16-7.13 (t, 2H), 7.03 (s, 1H), 6.82 (s, 1H), 6.73-6.71 (d, 2H).

Synthesis of 9-(7-bromo-9,9'-spirobi[fluorene]-2-yl)-3,6-ditertbutyl-9H-carbazole (5): Copper(I) iodide (18 mg, 0.1 mmol), 18-crown-6 (8.6 mg, 0.03 mmol), potassium carbonate

(0.526 g, 3.84 mmol), 3,6-ditertbutylcarbazole (0.536 g, 1.92 mmol), and DMAc (7.5 mL) were added to a round-bottom flask and vigorously stirred at 165 °C under argon. After stirring and refluxing for 2 h, 2-bromo-7-iodo-9,9'-spirobi[fluorene] (1.0 g, 1.92 mmol) as a solution in hot DMAc (7.5 mL) was added into the mixture slowly. The final reaction medium was heated to reflux for 24 h. The reaction solution was poured into water (300 mL), the precipitate was collected by filtration, dried and purified by column chromatography over silica gel eluting with a mixture of dichloromethane:*n*-hexane (1:4) followed by recrystallization from a mixture of dichloromethane-methanol gave a white solid (0.9 g, 70%). ¹H NMR (400 MHz, CDCl₃, 25 °C, TMS): δ (ppm) = 8.04-7.97 (dd, 3H), 7.81-7.74 (t, 3H), 7.55-7.52 (td, 2H), 7.39-7.33 (t, 4H), 7.18-7.12 (m, 4H), 6.91-6.89 (dd, 2H), 6.85-6.82 (d, 2H), 1.40 (s, 18H).

Synthesis of 3,6-di-tert-butyl-9-[7-(2-thienyl)-9,9'-spirobi[fluoren]-2-yl]-9H-carbazole (TCFT): A mixture of **5** (0.67 g, 1 mmol), 2-thiopheneboronic acid (0.14 g, 1.1 mmol), Pd(PPh₃)₄ (0.026 g, 0.026 mmol), aqueous solution of 2 M Na₂CO₃ (15 mL, 30.00 mmol) and THF (25 mL) was degassed with argon for 5 minute. The reaction mixture was stirred at reflux under Ar for 24 h. After being cooled to room temperature water (100 mL) was added. The mixture was extracted with dichloromethane (2×50 mL), washed with water (100 mL) and brine (100 mL), dried over anhydrous Na₂SO₄, filtered and the solvents were removed under vacuum. Purification by column chromatography over silica gel eluting with a mixture of dichloromethane: *n*-hexane (1:2) afforded white solids (0.58 g, 87 %). ¹H NMR (400 MHz, CDCl₃, 25 °C, TMS): δ (ppm) = 8.05-7.99 (dd, 4H), 7.89-7.88 (d, 1H), 7.82-7.80 (d, 1H), 7.37-7.31 (t, 4H), 7.19-7.11 (m, 8H), 7.00-6.97 (t, 2H), 6.89-6.87 (d, 2H), 1.41 (s, 18H); ¹³C NMR (100 MHz, CDCl₃, 25 °C, TMS): δ (ppm) = 151.36, 148.28, 144.46, 143.01, 142.03, 140.08, 139.20, 134.48, 128.23, 126.35, 124.94, 124.24, 123.71, 123.53, 121.72, 121.17, 120.70, 120.46, 116.39, 109.28, 32.21; IR (ATR): ν = 3039, 2953, 2351, 1605, 1471, 1446, 1360, 1324, 1293, 1251, 1231, 875, 809, 732 cm⁻¹; MALDI-TOF (m/z): [M⁺] calcd. for C₄₉H₄₁NS, 675.9226; found 675.3000.

Synthesis of 9-(7-bromo-9,9'-spirobi[fluoren]-2-yl)-9H-carbazole (6): Copper(I) iodide (0.056 g, 0.3 mmol), 18-crown-6 (0.026 g, 0.1 mmol), potassium carbonate (1.58 g, 11.52 mmol), carbazole (0.96 g, 5.76 mmol), and DMAc (10 mL) were added to a round-bottom flask and vigorously stirred at 165 °C under argon. After stirring and refluxing for 2 h, 2-bromo-7-iodo-9,9'-spirobi[fluorene] (3 g, 5.76 mmol) as a solution in hot DMAc (10 mL) was added into the mixture slowly. The final reaction medium was heated to reflux for 24 h. The reaction solution was poured into water (300 mL), the precipitate was collected by filtration,

dried and purified by column chromatography over silica gel eluting with a mixture of dichloromethane:*n*-hexane (1:4) followed by recrystallization from a mixture of dichloromethane-methanol gave a white solid (2.25 g, 70%). ¹H NMR (400 MHz, CDCl₃, 25 °C, TMS): δ (ppm) = 8.04-7.99 (dd, 3H), 7.80-7.74 (t, 3H), 7.58-7.53 (td, 2H), 7.39-7.35 (t, 2H), 7.29-7.24 (t, 2H), 7.21-7.15 (m, 6H), 6.92-6.89 (dd, 2H), 6.86-6.84 (d, 2H). MALDI-TOF (m/z): [*M*⁺] calcd. for C₃₇H₂₂BrN, 560.4813; found 561.0900.

Synthesis of 9-[7-(2-thienyl)-9,9'-spirobi[fluoren]-2-yl]-9H-carbazole (CFT): A mixture of **6** (1 g, 1.78 mmol), 2-thiopheneboronic acid (0.25 g, 1.95 mmol), Pd(PPh₃)₄ (0.047 g, 0.047 mmol), aqueous solution of 2 M Na₂CO₃ (20 mL, 40.00 mmol) and THF (20 mL) was degassed with argon for 5 min. The reaction mixture was stirred at reflux under Ar for 24 h. After being cooled to room temperature water (100 mL) was added. The mixture was extracted with dichloromethane (2×50 mL), washed with water (100 mL) and brine (100 mL), dried over anhydrous Na₂SO₄, filtered and the solvents were removed under vacuum. Purification by column chromatography over silica gel eluting with a mixture of dichloromethane: *n*-hexane (1:2) afforded white solids (0.89 g, 89 %). ¹H NMR (400 MHz, CDCl₃, 25 °C, TMS): δ (ppm) = 8.04-8.01 (t, 3H), 7.91-7.89 (d, 1H), 7.81-7.80 (d, 2H), 7.70-7.67 (dd, 1H), 7.57-7.55 (dd, 1H), 7.38-7.34 (t, 2H), 7.28-7.24 (t, 2H), 7.21-7.14 (m, 8H), 7.02 (s, 1H), 6.96-6.94 (t, 1H), 6.90-6.88 (d, 3H); ¹³C NMR (100 MHz, CDCl₃, 25 °C, TMS): δ (ppm) = 151.23, 149.85, 147.96, 144.14, 141.78, 140.60, 140.41, 140.25, 140.01, 137.08, 134.40, 128.03, 127.88, 126.43, 125.80, 124.76, 123.99, 123.33, 123.28, 122.10, 121.51, 120.55, 120.22, 119.82, 109.64; IR (ATR): ν = 3048, 2350, 1596, 1494, 1468, 1446, 1333, 1311, 1227, 814, 744, 719 cm⁻¹; MALDI-TOF (m/z): [*M*⁺] calcd. for C₄₁H₂₅NS, 563.7099; found 563.1700.

Synthesis of 9-(7-{5-[7-(9H-carbazol-9-yl)-9,9'-spirobi[fluoren]-2-yl]-2-thienyl}-9,9'-spirobi[fluoren]-2-yl)-9H-carbazole (CFTFC): A mixture of **6** (1 g, 1.78 mmol), 2,5-thiophenediboronic acid (0.154 g, 0.9 mmol), Pd(PPh₃)₄ (0.047 g, 0.047 mmol), aqueous solution of 2 M Na₂CO₃ (20 mL, 40.00 mmol) and THF (20 mL) was degassed with argon for 5 minute. The reaction mixture was stirred at reflux under Ar for 24 h. After being cooled to room temperature water (100 mL) was added. The mixture was extracted with dichloromethane (2×50 mL), washed with water (100 mL) and brine (100 mL), dried over anhydrous Na₂SO₄, filtered and the solvents were removed under vacuum. Purification by column chromatography over silica gel eluting with a mixture of dichloromethane: *n*-hexane (1:2) afforded pale green solids (0.74 g, 80 %). ¹H NMR (400 MHz, CDCl₃, 25 °C, TMS): δ (ppm) = 8.05-8.02 (t, 5H), 7.92-7.90 (d, 2H), 7.82-7.80 (d, 3H), 7.70-7.68 (d, 2H), 7.58-7.56

(d, 2H), 7.39-7.35 (t, 4H), 7.30-7.26 (t, 4H), 7.21-7.15 (m, 15H), 7.02 (s, 2H), 6.98-6.95 (t, 2H), 6.90-6.88 (d, 5H); ^{13}C NMR (100 MHz, CDCl_3 , 25 °C, TMS): δ (ppm) = 151.49, 150.10, 148.21, 147.58, 144.40, 142.03, 140.86, 137.33, 134.65, 131.43, 128.28, 128.25, 126.35, 126.06, 125.01, 124.24, 123.59, 122.85, 121.77, 121.28, 120.47, 120.08, 109.89; IR (ATR): ν = 3051, 2350, 1596, 1494, 1445, 1334, 1312, 1229, 1116, 810, 746, 722 cm^{-1} ; MALDI-TOF (m/z): [M^+] calcd. for $\text{C}_{78}\text{H}_{46}\text{N}_2\text{S}$, 1043.2793; found 1042.3400.

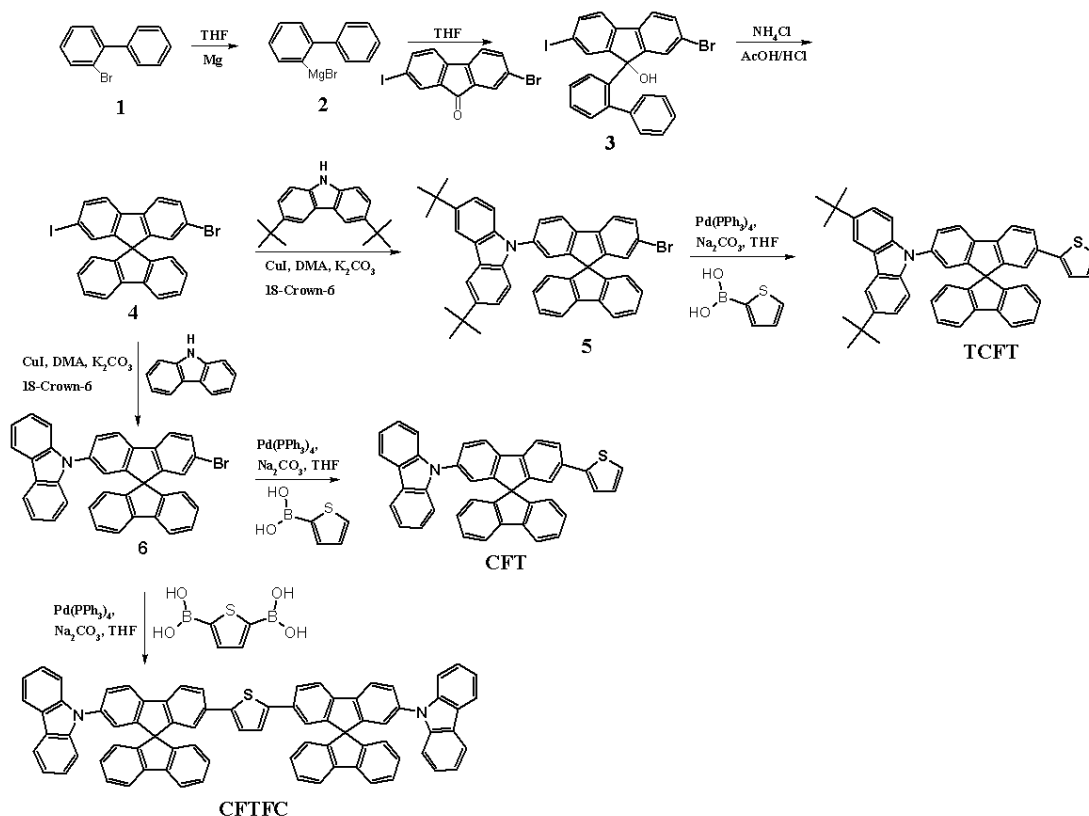
OLED Device Fabrication and Characterization

Indium tin oxide (ITO) glass substrate with a sheet resistance of 15 Ω/sq was used. After cleaning of ITO glass substrate in an ultrasonic bath with acetone, ethanol, *iso*-propanol for 15 min., PEDOT:PSS was spin coated onto the substrate at a spin speed of 4000 rpm for 30 s forming 40 nm thick layers. The samples were annealed for 30 min at 150 °C. Chlorobenzene solutions of synthesized molecules and PVK (1.5%, w/v) were spin-coated onto ITO glass substrates at a spin speed of 3000 rpm for 60 s to get a 50 nm thick of HTL. Then Alq3 was deposited onto the surface of the synthesized molecules films as emissive layer (EML) and electron transporting layer (ETL) with a thickness of 20 nm. Finally, an ultra thin LiF layer (0.5 nm) and Al cathode (100 nm) was thermally evaporated under high vacuum (10^{-6} mbar) through a shadow mask determining the active surface area of 10 mm^2 . The characterization of fabricated devices was carried out under inert nitrogen environment inside a glove box system. Current-voltage (IV) curves were recorded using a Keithley 236 source meter. The EL and luminance properties were measured using Spectrascan PR-655 spectroradiometer. The thicknesses of films were determined with a Digital Instrument 3100 atomic force microscope (AFM).

Results and Discussion

Synthesis and Characterization

The synthetic routes of CFT, TCFT and CFTFC molecules are shown in Scheme 1. 2-bromo-7-iodo-9,9'-spirobi[fluorene] was prepared according to procedures previously described in literatures.²⁹ Coupling of 2-bromo-7-iodo-9,9'-spirobi[fluorene] with carbazole or 3,6-ditert-butyl carbazole under Ullmann coupling reaction conditions gave 5 and 6. CFT and TCFT molecules were obtained coupling of the intermediate 5 or 6 with 2-thiopheneboronic acid under palladium catalyzed Suzuki cross-coupling conditions in good yield. CFTFC molecule was synthesized under Suzuki cross-coupling conditions coupling of 6 with 2,5-thiophenediboronic acid.



Scheme 1. Synthesis of TCFT, CFT and CFTFC molecules.

All the synthesized compounds were characterized by ^1H , ^{13}C NMR, FT-IR spectroscopy and MALDI-TOF. The data were found to be in good agreement with the proposed structures. CFT, TCFT and CFTFC molecules are highly soluble in common organic solvents such as chloroform, chlorobenzene, tetrahydrofuran and toluene at room temperature.

The thermal properties of the compounds were determined by DSC and TGA under nitrogen atmosphere with a heating rate of $10\text{ }^\circ\text{C min}^{-1}$ and in the temperature range between 0 and $275\text{ }^\circ\text{C}$ for DSC and between 25 and $700\text{ }^\circ\text{C}$ for TGA. DSC and TGA data revealed that all compounds have high glass transition (T_g) and thermal decomposition temperatures (T_d) indicating that they are thermally stable materials (Table 1). There is no observed exothermic peak resulting from the crystallization of compounds up to $275\text{ }^\circ\text{C}$ in their DSC curves. As shown in Table 1, sterically bulky tert-butyl groups linked to carbazole moieties increase the T_g and T_d of TCFT molecules relative to the analog CFT. Additional spirobifluorene and carbazole groups in CFTFC proved to have almost no effect on the thermal properties of the molecule.

Table 1. Physical data for compounds

| Compound | T_g^a [°C] | T_d^b [°C] | λ_{abs}^c [nm] | λ_{em}^c [nm] | E_g^d [eV] | E_{onset}^e [eV] | HOMO/LUMO ^f [eV] |
|----------|-----------------|-----------------|---------------------------|--------------------------|-----------------|-----------------------|--------------------------------|
| CFT | 135 | 461 | 346 | 384/397 | 3.12 | 1.20 | -5.59/-2.47 |
| TCFT | 145 | 490 | 351 | 391 | 3.08 | 1.29 | -5.68/-2.60 |
| CFTFC | 135 | 452 | 343 | 383/394 | 3.05 | 1.28 | -5.67/-2.62 |

^[a]Obtained from DSC measurements. ^[b]Obtained from TGA measurements. ^[c]Solvent CHCl₃. ^[d]Optical band gap (thin film). ^[e]Onset potentials. ^[f]HOMO/LUMO energy levels was calculated with reference to ferrocene (4.8 eV) according to onset potentials. LUMO energy level was derived from the relation, $E_g = \text{HOMO} - \text{LUMO}$ (where the band gap was derived from the observed optical edge).

The absorption spectra and photoluminescence spectra of CFT, TCFT and CFTFC were recorded in chloroform (Fig. 1). In the absorption spectra of all compounds, there is no significant shift in comparison to the spectrum of the carbazole subchromophore (*N*-phenyl carbazole, $\lambda_{max} = 340$ nm). The UV-vis spectra have absorption maxima between 343 and 351 nm, which are assigned to the $\pi-\pi^*$ transitions of the carbazole moiety. A comparison of the spectra shows that CFT and CFTFC compounds exhibit almost identical spectral features despite of the different molecular structures. Tert-buthyl substitution in TCFT causes a redshift of the absorption maximum. The energy band gap (E_g) of CFT, TCFT and CFTFC were estimated from thin film absorption edge as 3.12, 3.08 and 3.05 eV, respectively. The solution photoluminescence (PL) spectra of molecules showed emission bands in the purple-blue region with peaks centered between 383 and 397 nm. CFT and CFTFC exhibited almost identical PL spectra same as their UV-vis spectra and PL spectra of TCFT presented slight redshift of emission maximum. Due to the steric effect of the two *tert*-butyl groups at the 3,6-position of the carbazole, the absorption and emission bands of TCFT are bathochromically shifted, relative to CFT and CFTFC.

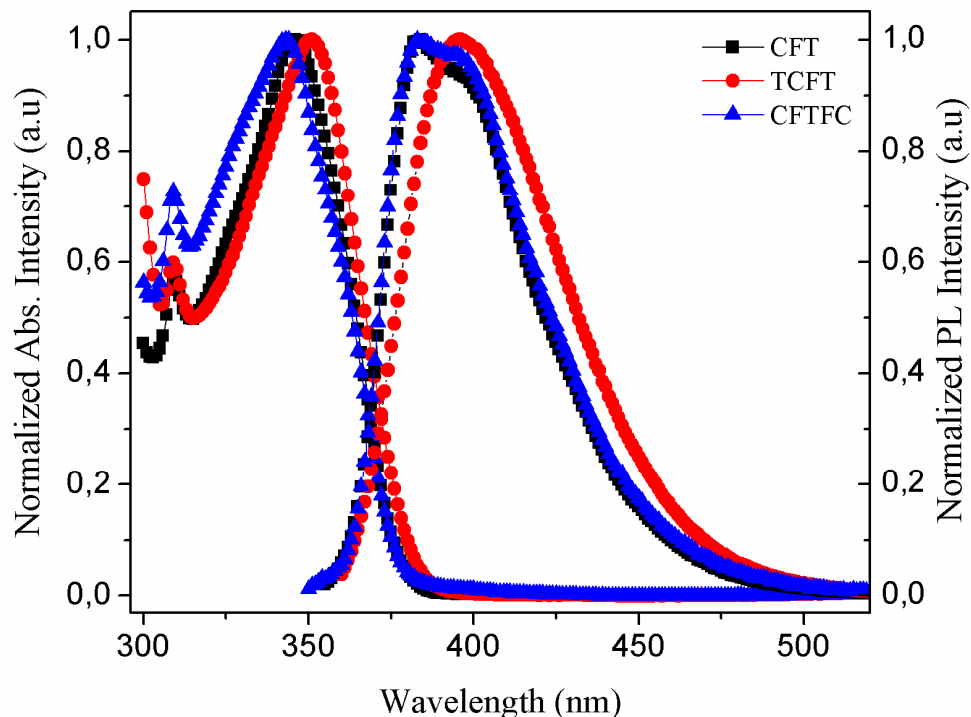


Fig. 1 Normalized UV-Vis absorption and Photoluminescence spectra of CFT, TCFT and CFTFC molecules in chloroform solution.

Cyclic voltammetry was used to determine the position of the highest occupied molecular orbital (HOMO) of CFT, TCFT and CFTFC molecules (Table 1). CV experiment was carried out in degassed anhydrous acetonitrile-dichloromethane (2:1, v:v) solutions. HOMO energy levels of molecules were calculated according to the inner reference ferrocene redox couple $E^{\circ}(\text{Fc}/\text{Fc}^+) = +0.41 \text{ V vs. Ag/AgCl}$ in acetonitrile by using the formula $E_{\text{HOMO}} = -e(E_{\text{ox}} - E_{\text{Fc}}) + 4.8$.³⁰ The first oxidation peaks of CFT, TCFT and CFTFC were observed at 1.20, 1.29 and 1.28 V, respectively against (vs. Ag/AgCl). Lowest unoccupied molecular orbital (LUMO) energy levels of CFT, TCFT and CFTFC molecules were obtained by adding their optical band gap values to their HOMO levels, and they are calculated as -2.47, -2.60 and -2.62 eV, respectively. The energy level diagram of HOMO and LUMO levels for materials are shown in Fig. 2.

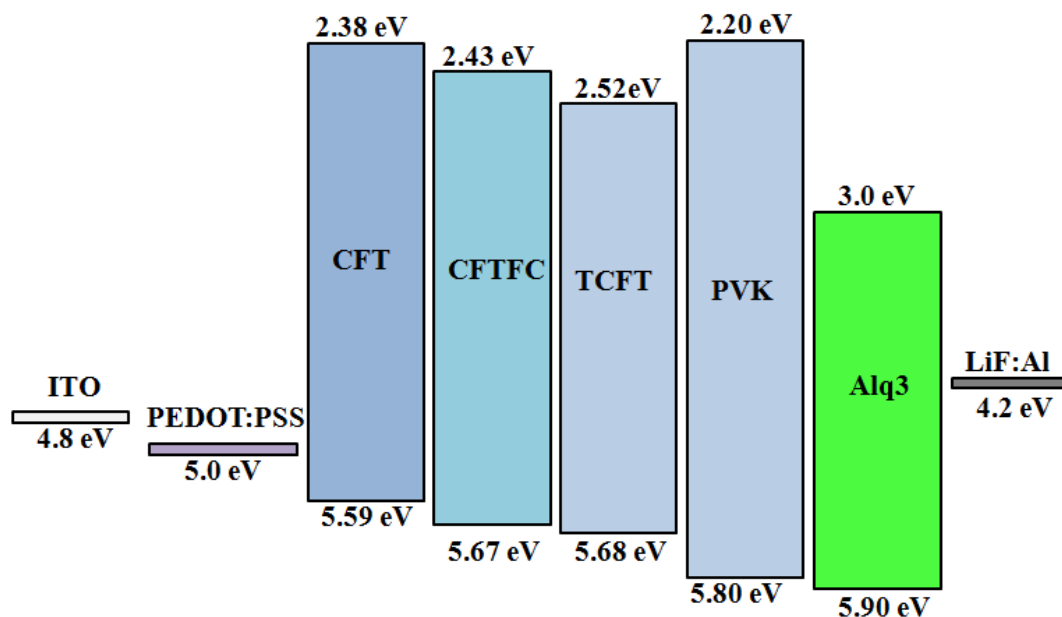


Fig. 2 Energy level diagram of the fabricated OLED devices.

Electroluminescence Properties

To investigate the hole-transporting properties of CFT, TCFT and CFTFC molecules, OLED devices were fabricated with the device configuration of ITO/PEDOT:PSS/HTL/Alq₃/LiF:Al (Fig. 3). In this device configuration CFT, TCFT and CFTFC were used as HTL materials, Alq₃ was used both as a light emitting and ETL material, ITO and LiF:Al were used as an anode and cathode, respectively. A reference device based on ITO/PEDOT:PSS/PVK/Alq₃/LiF:Al was fabricated for comparison.

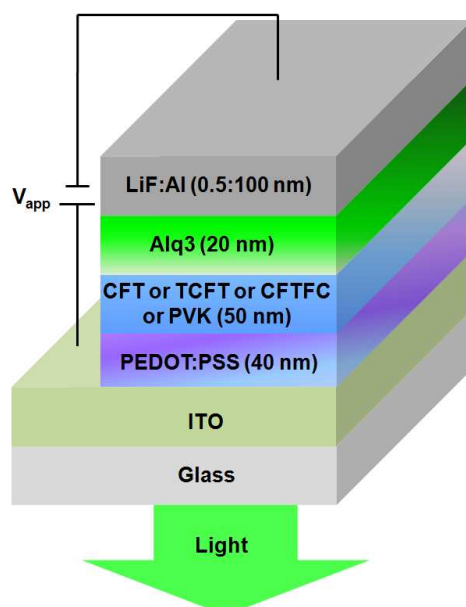


Fig. 3 General structure of ITO/PEDOT:PSS/CFT or TCFT or CFTFC or PVK/Alq3/LiF:Al OLED devices.

EL spectra of the all devices are shown in Fig. 4. All devices emitted bright green luminescence ($\lambda_{\text{max}} = 512\text{-}520\text{ nm}$) in agreement with the PL spectrum of Alq3. Fig. 4 clearly shows that, in all devices, charge recombinations occurred in Alq3 layer. No emission at the longer wavelength from the exciplex species formed at the interface of HTL and ETL materials were observed from their OLED devices, which generally occurs in the devices containing planar molecules as HTL.

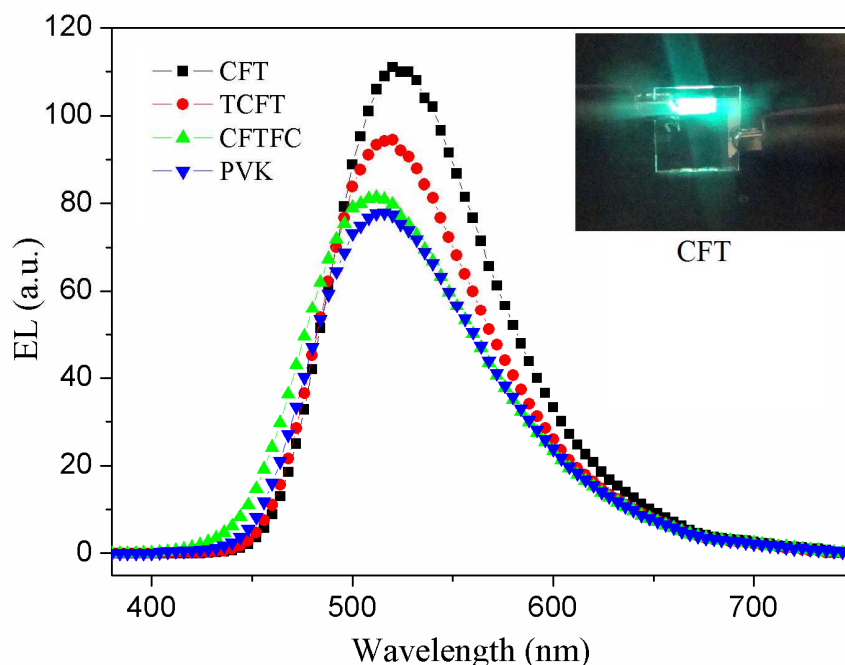
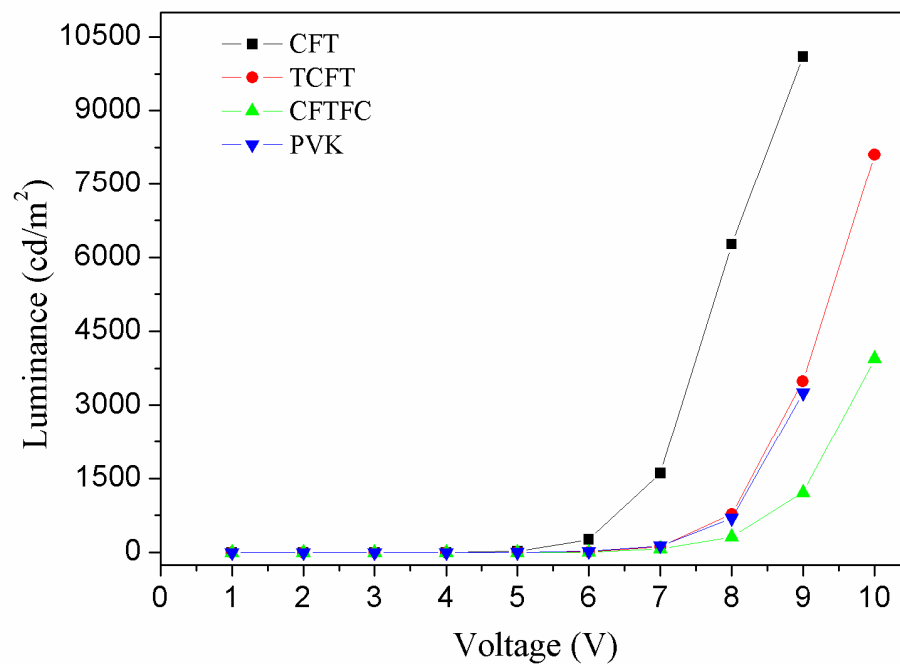
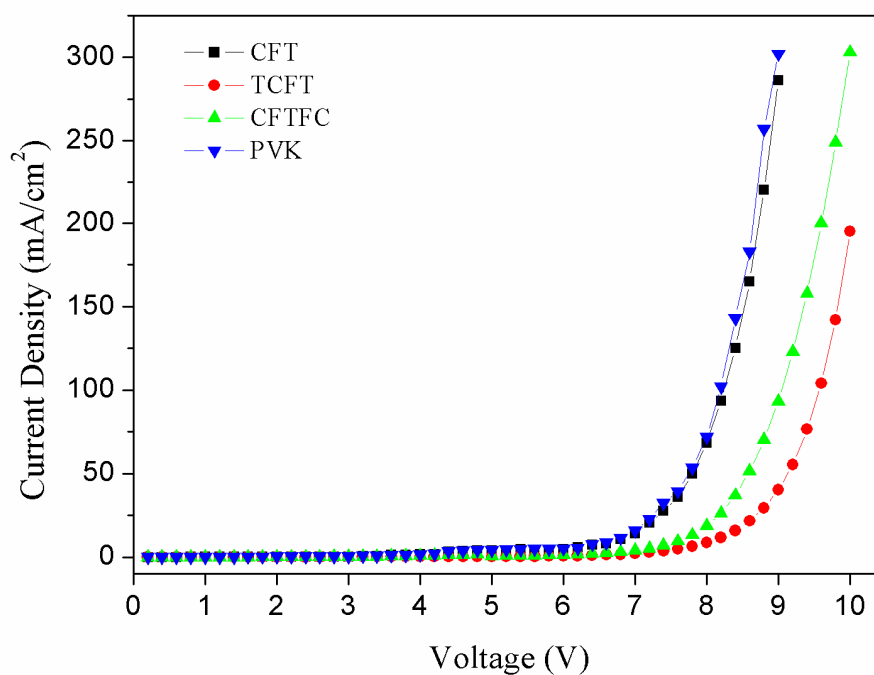


Fig. 4. EL spectrum of the OLED devices.

Fig. 5 shows the current-voltage and luminance-voltage characteristics of the OLED devices containing the CFT, TCFT, CFTFC and PVK molecules as HTMs. The electrical parameters obtained from OLED devices with different HTMs are summarized in Table 2. Luminance-voltage characteristics clearly show that OLED device based on CFT exhibit the lowest turn-on voltages to obtain the luminance of 1 cd/m^2 as 3V and a maximum luminances of 10100 cd/m^2 at 9 V, which can be due to better energy level alignment of CFT HOMO level with respect to PEDOT:PSS as compared to TCFT, CFTFC and PVK, as charge injection barrier is one of the determining parameters of turn on voltage in OLED devices.



a)



b)

Fig. 5. (a) Luminescence-applied voltage characteristics and (b) Current density-applied voltage characteristics of the OLED devices.

Table 2. EL Performance of fabricated OLED devices.

| Device | V_{on} (V) ^a | λ_{EL} (nm) | L_{max} (cd/m ²) ^b | J (mA/cm ²) ^c | η (cd/A) ^d | CIE (x,y) ^e |
|----------------------------------|-------------------------------------|-------------------------------|---|---|-------------------------------|---------------------------|
| ITO/PEDOT:PSS/CFT/Alq3/ LiF:Al | 3 | 520 | 10100 | 286 | 11.30 | 0.30, 0.56 |
| ITO/PEDOT:PSS/TCFT/Alq3/ LiF:Al | 4 | 520 | 8100 | 195 | 9.01 | 0.29, 0.55 |
| ITO/PEDOT:PSS/CFTFC/Alq3/ LiF:Al | 5 | 512 | 4000 | 303 | 1.84 | 0.28, 0.54 |
| ITO/PEDOT:PSS/PVK/Alq3/ LiF:Al | 4 | 516 | 3250 | 302 | 1.08 | 0.29, 0.51 |

^aTurn-on voltage (V), recorded at luminance of 1 cd/m².

^bMaximum luminance (cd/m²).

^cCurrent density at maximum luminance.

^dLuminance efficiency.

^eCIE coordinates (x, y).

Molecular structure can affect intermolecular interactions ie. hole transport properties in these molecules. TCFT has sterically bulky tert-butyl groups linked to carbazole moieties and CFTFC has two spirobifluorene groups, leading to twisted molecular structure thus minimizing molecular packing. This can be the reason for lower performances in OLED devices coming from their relatively poor hole transport abilities comparing to CFT.

Fig. 6 shows luminous efficiency-current density characteristics of fabricated devices. According to this figure, all synthesized molecules have higher luminance and current efficiency value than the reference ITO/PEDOT:PSS/PVK/Alq3/LiF:Al device. Maximum luminous efficiency of 11.32 cd/A was achieved at 13 mA/cm² by incorporating CFT. This excellent performance of CFT can be attributed to its better energy level alignment with PEDOT:PSS as well as improved hole transport property.

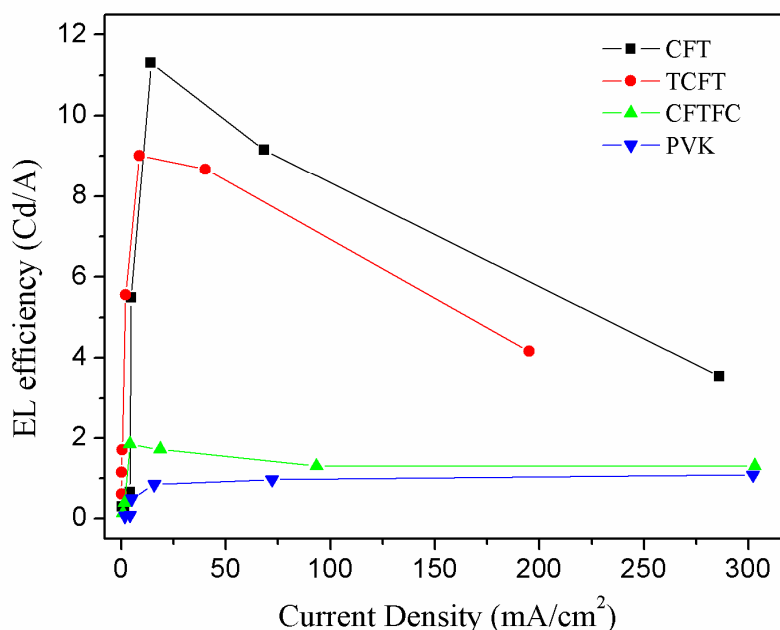


Fig. 6. The luminous efficiency-current density characteristics of the OLED devices.

Conclusion

In summary, we have synthesized electrochemically and thermally stable new spirobifluorene based hole transporting materials by Ulmann coupling and Suzuki Cross-coupling reactions. The OLED devices using these molecules as hole transporting layer exhibited bright green emission ($\lambda_{\max} = 512\text{-}520$ nm) from the Alq3 layer. The device based on CFT molecules containing carbazole, spirobifluorene and thiophene has much better performance in terms of brightness, current density and current efficiency than other devices based on TCF, CFTFC and as well as reference PVK devices due to its better energy level alignment with PEDOT:PSS and good hole transport property. This molecule can be a promising material for display applications that renders high EL efficiency in OLEDs with its excellent hole transporting ability.

Acknowledgements

The author would like to thank Prof. Niyazi Serdar Sariciftci for providing research facilities for device fabrication and characterization at Linz Institute for Organic Solar Cells. The author is also grateful to the Mugla Sıtkı Kocman University (BAP Project 2012/138) for financial support.

References

- 1 S. A. Jenekhe, *Adv. Mater.*, 1995, 7, 309.
- 2 C.H. Chen, J. Shi, C.W. Tang, *Coord. Chem. Rev.*, 1998, 171, 161.
- 3 F. Hide, M. A. Diaz-Garcia, B. J. Scharzt, A. J. Heeger, *Acc. Chem. Res.*, 1997, 30, 430.
- 4 U. Mitschke, P. Bauerle, *J. Mater. Chem.*, 2000, 10, 1471.
- 5 C. W. Tang, S. A. Van Slyke, *Appl. Phys. Lett.*, 1987, 51, 913.
- 6 J. H. Burroughes, D. D. C. Bradley, A. R. Brown, R. N. Marks, K. Mackay, R. H. Friend, P. L. Burn, A. B. Holmes, *Nature*, 1990, 347, 539.
- 7 U. Scherf, E. J. W. List, *Adv. Mater.*, 2002, 14, 477.
- 8 N. C. Greenham, S. C. Moratti, D. D. C. Bradley, R. H. Friend, P. L. Burn, A. B. Holmes, *Nature*, 1993, 365, 628.
- 9 L. S. Liao, K. P. Klubeck, C. W. Tang, *Appl. Phys. Lett.*, 2004, 84, 167.
- 10 a) Ö. Usluer, S. Demic, M. Kus, F. Özel, N. S. Sariciftci, *Journal of Luminescence*, 2014, 146, 6; b) S. Koyuncu, O. Usluer, M. Can, S. Demic, S. Icli, N. S. Sariciftci, *J. of Mater. Chem.*, 2011, 21, 2684; c) X. Chen, J. L. Liao, Y. Liang, M. O. Ahmed, H. E. Tseng, S. A. Chen, *J Am Chem Soc*, 2002, 125, 636.
- 11 a) M. Svensson, F. L. Zhang, S. C. Veenstra, W.J. H. Verhees, J. C. Hummelen, J. M. Kroon, O. Inganas, M. R. Andersson, *Adv Mater*, 2003, 15, 988; b) C. R. McNeill, J. J. M. Halls, R. Wilson, G. L. Whiting, S. Berkebile, M. G. Ramsey, R. H. Friend, N. C. Greenham, *Adv Funct Mater*, 2008, 18, 2309.
- 12 a) M. Chen, X. Crispin, E. Perzon, M. R. Andersson, T. Pullerits, M. Andersson, O. Inganas, M. Berggren, *Appl Phys Lett*, 2005, 87, 252105; b) E. Lim, Y. M. Kim, J.-I. Lee, B.-J. Jung, N. S. Cho, J. Lee, L.-M. Do, H.-K. Shim, *J Polym Sci Part A: Polym Chem* 2006, 44, 4709.
- 13 a) J. Krueger, R. Plass, M. Gratzel, P. J. Cameron, L. M. J. Peter, *J. Phys. Chem. B*, 2003, 107, 7536; b) P. A. Marcos, J. A. Alonso, L. M. Molina, A. Rubio, M. J. Lopez, *J. Chem. Phys.*, 2003, 119, 1127.
- 14 D. T. Chase, A. G. Fix, S. J. Kang, B. D. Rose, C. D. Weber, Y. Zhong, L. N. Zakharov, M. C. Lonergan, C. Nuckolls, M. M. Haley, *J. Am. Chem. Soc.*, 2012, 134, 10349.
- 15 a) A.W. Grice, D. D. C. Bradley, M. T. Bernius, M. Indasekaran, W. W. Wu, E. P. Woo, *Appl Phys Lett*, 1998, 73, 629; b) S. Janietz, D. D. C. Bradley, M. Grell, C. Giebeler, M. Inbasekaran, E. P. Woo, *Appl Phys Lett*, 1998, 73, 2453.
- 16 G. Klarner, R. D. Miller, *Macromolecules*, 1998, 31, 2007.

- 17 S. A. Jenekhe, J. A. Osaheni, *Science*, 1994, 265, 765; (b) M. Grell, D. D. C. Bradley, G. Ungar, J. Hill, K. S. Whitehead, *Macromolecules*, 1999, 32, 5810.
- 18 a) W.-L. Yu, J. Pei, W. Huang, A. J. Heeger, *Adv. Mater.*, 2000, 12, 828; b) C. D. Mueller, A. Falcou, N. Reckefuss, M. Rojahn, V. Wiederhirn, P. Rudati, H. Frohne, O. Nuyken, H. Becker, K. Meerholz, *Nature*, 2003, 421, 829; c) K.-T. Wong, Y.-Y. Chien, R.-T. Chen, C.-F. Wang, Y.-T. Lin, H.-H. Chiang, P.-Y. Hsieh, C.-C. Wu, C. H. Chou, Y. O. Su, G.-H. Lee, S.-M. Peng, *J. Am. Chem. Soc.* 2002, 124, 11576.
- 19 a) R. Wu, J. S. Schumm, D. L. Pearson, J. M. Tour, *J Org Chem*, 1996, 61, 6906; b) Y. H. Kim, D. C. Shin, S. H. Kim, C. H. Ko, H. S. Yu, Y. S. Chae, S. K. Kwon, *Adv. Mater.*, 2001, 13, 1690; c) D. C. Shin, Y. H. Kim, H. You, S. K. Kwon, *Macromolecules*, 2003, 36, 3222.
- 20 K. R. Justin Thomas, J. T. Lin, Y. T. Tao, C. W. Ko, *J. Am. Chem. Soc.*, 2001, 123, 9404.
- 21 H. Y. Fu, H. R. Wu, X.Y. Hou, F. Xiao, B. X. Shao, *Synth. Met.*, 2006, 156, 809.
- 22 M.-H. Ho, B. Balaganesan, T. Chu, T. Chen, C. H. Chen, *Thin Solid Films*, 2008, 517, 943.
- 23 a) O. Usluer, S. Demic, D. A. M. Egbe, C. Birckner, C. Tozlu, A. Pivrikas, A. M. Ramil, N. S. Sariciftci, *Adv. Funct. Mater.*, 2010, 20, 4152; b) N. Prachumrak, S. Pansay, S. Namuangruk, T. Kaewin, S. Jungsuttiwong, T. Sudyoasuk, V. Promarak, *Eur. J. Org. Chem.*, 2013, 6619.
- 24 W. Li, J. Qiao, L. Duan, L. Wang, Y. Qiu, *Tetrahedron*, 2007, 63, 10161.
- 25 J. Ding, J. Gao, Y. Cheng, Z. Xie, L. Wang, D. Ma, X. Jing, F. Wang, *Adv. Funct. Mater.*, 2006, 16, 575.
- 26 K. R. Thomas, J. T. Lin, Y. T. Tao, C. Ko, *J. Am. Chem. Soc.*, 2001, 123, 9404.
- 27 M. Guan, Z. Chen, Z. Bian, Z. Liu, G. Gong, W. Baik, H. Lee, C. Huang, *Org. Electron.*, 2006, 7, 330.
- 28 Y. Liu, M. Nishiura, Y. Wang, Z. Hou, *J. Am. Chem. Soc.*, 2006, 128, 5592.
- 29 J. Pei, J. Ni, X. H. Zhou, X. Y. Cao, *J. Org. Chem.*, 2002, 67, 4924.
- 30 a) G. Yu, Y. Yang, Y. Cao, Q. Pei, C. Zhang, A. J. Heeger, *Chem. Phys. Lett.*, 1996, 259, 465; b) A. Berlin, G. Zotti, S. Zecchin, G. Schiavon, B. Vercelli, A. Zanelli, *Chem. Mater.*, 2004, 16, 3667.